Nonlinear thermal convection on unsteady thin film flow with variable properties

M. Karuna Prasad[1], Naveenkumar S H [2] ,C. S. K. Raju[3*], S. Mamatha Upadhya [4]

[1,2] Department of Mathematics, GITAM Deemed to be University, Bengaluru-Campus, Nagadenahalli, Karnataka, India.

[3*] Department of Mathematics, GITAM Deemed to be University, Bengaluru-Campus, Nagadenahalli, Karnataka, India.

[4] Department of Mathematics, Kristu Jayanti College, Autonomous, PO, K.Narayanapura, Kothanur, Bengaluru, Karnataka-560077, India.

Email: karunaprasad9@gmail.com[1], naveenkumarsh.220@gmail.com[2], sivaphd90@gmail.com[3], mamathasupadhya@gmail.com[2]

Abstract.This study portray the influence of variable viscosity, thermocapillarity, nonlinear convection , variable thermal conductivity on the laminar flow and heat transfer in a liquid film on a horizontal stretching sheet. Time dependent flow equations are transformed to coupled ordinary equations by the assistance of similarity transformation. Numerical results are obtained via applying Runge-kutta and Newton's methods. For some representative value of the parameters graphs are exhibited and surface skin friction coefficient and heat transfer are presented in tabular form. It is observed that non-linear convection case shows higher velocity and associated boundary layer thickness compared with linear convection. Elapsed time is more in nonlinear convection for growing values of $A, \delta, \Pr$ and M compared to linear convection.

1. Introduction

Analysis of flows due to a stretching of a boundary with heat transfer has captivated the curiosity of the research community due to their widespread applications in extrusion process, manufacturing of rubber, plastic sheets, glass blowing, food processing, polymer processing etc. Crane [1] initiated the study of boundary layer two- dimensional flow of steady viscous fluid over a stretching surface. He modeled the exact similarity solution in closed analytical form. Hayat et al. [2] studied impact of cattaneo-christov heat flux with variable thickness on the flow over a stretching sheet. Rashid et al. [3] investigated buoyancy effect on the MHD flow over a stretching sheet along with thermal radiation. Majeed et al. [4] studied heat transfer in ferromagnetic viscoelastic fluid flow with suction over a stretching sheet. Takhar et al. [5] made an analysis of the flow and mass transfer of viscous electrically conducting fluid with non-zero slot velocity on a continuously stretching surface. Raju et al. [6] investigated cross-diffusion effects, radiation and inclined magnetic field effects on flow over the stretching surface. Aziz [7] studied mixed convection flow of micropolar fluid with viscous dissipation from an unsteady stretching surface. Thus,

umpteen number of literature is found discussing boundary layer flow over a stretching sheet considering steady and unsteady case in literature [8-15].

In all these boundary layer flow investigations, boundary conditions are considered at the sheet and on the fluid at infinity. During 1990, Wang [16] investigated hydrodynamics of the flow of liquid film on an unsteady stretching surface. Currently, Aziz et al. [17] analyzed thin film nanofluid flow on an unsteady stretching sheet. They considered three different types of nanoparticles such as Cu, Al_2O_3, TiO_2 and observed that heat transfer rate declines with increase in volume fraction of nanoparticles. Faraz et al. [18] studied thin film flow of Maxwell fluid over stretching/shrinking sheet. Dandapat et al. [19] discussed on the flow of thin film the influence of variable fluid properties and thermocapillarity. Khader [20] numerically investigated unsteady thin film flow considering magnetic field and thermal radiation. Sandeep [21] discussed influence of aligned magnetic field considering graphene nanoparticles on liquid thin film flow.

The nonlinear density temperature (NDT) discrepancy in the buoyancy force term play a major role in the mechanism of flow, heat and mass transfer especially in nuclear reactor safety, solar collectors and electronic cooling's. In view of this recently researchers Mamatha et al. [22], Shehzad et al. [23], Kumar et al. [24] and Qayyum et al. [25] studied effects of nonlinear convection in the flow of Newtonian and non-Newtonian fluid.

In this study, we analyze the unsteady boundary layer flow and heat transfer of thin film due to a stretching sheet the influence of nonlinear thermal convection, thermocapillarity, thermal conductivity and variable viscosity are discussed in detail.

2. Mathematical formulation

In the present theoretical model, a thin liquid film of uniform thickness $h(t)$ which lies on the horizontal sheet is considered. The fluid motion within the film is initially caused due to the stretching of the thin elastic sheet (see Figure. 1). The stretching sheet at $y=0$ moves with the velocity $\hat{U}=\dfrac{bx}{(1-\alpha)}$ (b and α are both positive constants) in its own plane. $\hat{T}_s = T_\circ - \left(\dfrac{1}{2}\right)\hat{T}_{ref}.(\mathrm{Re}_x)\left(\dfrac{1}{1-\alpha t}\right)$ the surface temperature of the sheet vary with the distance x from the slit. Here, $\mathrm{Re}_x = \dfrac{\hat{U}x}{v_\circ} = \dfrac{bx^2}{v_\circ(1-\alpha t)}$ is the local Reynolds number associated with the stretching sheet velocity $\hat{U}$. $\hat{T}_\circ$ represents temperature at the slit, $\hat{T}_{ref}\left(0 \le \hat{T}_{ref} \le T_\circ\right)$ represents constant reference temperature. In the present model variation of the

viscosity $(\mu_\circ)$, thermal conductivity $(k_\circ)$ and surface tension $(\sigma_\circ)$ with temperature are considered to be in the form;

$$\mu = \mu_\circ \left(e^{-\xi\left(\hat{T}-\hat{T}_\circ\right)} \right) \tag{1}$$

$$k = k_\circ \left(1 + c\left(\hat{T}-\hat{T}_\circ\right) \right) \tag{2}$$

$$\sigma = \sigma_\circ \left(1 - \gamma\left(\hat{T}-\hat{T}_\circ\right) \right) \tag{3}$$

In the thin liquid layer the velocity and temperature fields governed by the 2D boundary layer equations for mass, momentum and thermal energy takes the form: (See Dandapat et al. [19])

$$\frac{\partial \hat{u}}{\partial x} + \frac{\partial \hat{v}}{\partial y} = 0 \tag{4}$$

$$\frac{\partial \hat{u}}{\partial t} + \hat{u}\frac{\partial \hat{u}}{\partial x} + \hat{v}\frac{\partial \hat{u}}{\partial y} = \frac{1}{\rho_\circ}\frac{\partial}{\partial y}\left(\mu \frac{\partial \hat{u}}{\partial y} \right) + g\left(\beta\left(\hat{T}-\hat{T}_\circ\right) + \beta_1\left(\hat{T}-\hat{T}_\circ\right)^2 \right) \tag{5}$$

$$\frac{\partial \hat{T}}{\partial t} + \hat{u}\frac{\partial \hat{T}}{\partial x} + \hat{v}\frac{\partial \hat{T}}{\partial y} = \frac{1}{\rho_\circ c_p}\frac{\partial}{\partial y}\left(k \frac{\partial \hat{T}}{\partial y} \right) \tag{6}$$

The boundary conditions associated with the flow are:

$$at\ \ y = 0,\ \hat{u} = \hat{U},\ \ \hat{v} = 0,\ \ \hat{T} = \hat{T}_s \tag{7}$$

$$at\ \ y = h,\ \ \mu\frac{\partial \hat{u}}{\partial y} = \frac{\partial \sigma}{\partial x} \tag{8}$$

$$at\ \ y = h,\ \ \frac{\partial \hat{T}}{\partial y} = 0 \tag{9}$$

$$at\ \ y = h,\ \ \hat{v} = \frac{dh}{dt} \tag{10}$$

Here, g represents gravitational acceleration, β and β_1 linear and nonlinear thermal expansions coefficients.

Similarity transformation:

Dimensionless variables f and θ , similarity variable ζ are taken as :

$$\Psi = \left(\hat{v}_\circ b\left(1-\alpha t\right)^{-1} \right)^{1/2} x f\left(\zeta\right) \tag{11}$$

$$\hat{T} = \hat{T}_0 - \hat{T}_{ref}\left(bx^2 / 2\hat{v}_\circ \right)\left(1-\alpha t\right)^{(-3/2)}\theta\left(\zeta\right) \tag{12}$$

$$\zeta = \left(b/\hat{v}_\circ \right)^{(1/2)} (1-\alpha t)^{(-1/2)}\, y \tag{13}$$

Here, $\Psi(x, y, t)$ is the physical stream function, the velocity components are obtained as:

$$\hat{u} = \frac{\partial \Psi}{\partial y} = bx(1-\alpha t)^{-1} f'(\zeta) \tag{14}$$

$$\hat{v} = -\frac{\partial \Psi}{\partial x} = -\left(v_\circ b(1-\alpha t)^{-1} \right)^{(1/2)} f(\zeta) \tag{15}$$

With the similarity transformations the flow equations (1)-(7) are transformed as:

$$S\left(f'(\zeta) + \frac{\zeta}{2} f''(\zeta) \right) + \left(f'(\zeta) \right)^2 - f(\zeta) f''(\zeta) = \begin{pmatrix} e^{(A\theta(\zeta))} \left(f'''(\zeta) + A f''(\zeta) \theta'(\zeta) \right) \\ +\lambda \left(1 + \lambda_1 \theta(\zeta) \right) \theta(\zeta) \end{pmatrix} \tag{16}$$

$$\frac{S}{2}\left(3\theta(\zeta) + \zeta\theta'(\zeta) \right) + 2\theta(\zeta) f'(\zeta) - \theta'(\zeta) f(\zeta) = \begin{pmatrix} \left(\frac{1}{\Pr} \right) \left(1 - \delta\theta(\zeta) \right) \\ \theta''(\zeta) - \delta \left(\theta'(\zeta) \right)^2 \end{pmatrix} \tag{17}$$

$$f(0) = 0,\ f'(0) = 1,\ \theta(0) = 1 \tag{18}$$

$$f''(\beta) = M\theta(\beta) e^{-A\theta(\beta)} \tag{19}$$

$$f(\beta) = S\left(\beta/2 \right) \tag{20}$$

$$\theta'(\beta) = 0 \tag{21}$$

In the present transformed problem the boundary conditions are imposed at $\zeta = 0$ and $\zeta = \beta$ Here, $\hat{T} = \hat{T}_\circ + \theta(\zeta)\left(\hat{T}_s - \hat{T}_\circ \right), \delta = c\left(\hat{T}_\circ - \hat{T}_s \right)$ is the thermal conductivity parameter, $A = (-\xi)\left(\hat{T}_s - \hat{T}_\circ \right)$ (A is positive, as $T_\circ > T_s$) is the variable viscosity parameter, $S = \frac{\alpha}{b}$ is unsteadiness parameter, $\lambda = \frac{Gr}{\mathrm{Re}_x^2}$ is mixed convection parameter, $Gr = \frac{g\beta\left(\hat{T}_s - T_\circ \right) x^3}{v_\circ^2}$ is the Grashof number associated with temperature, $\lambda_1 = \frac{\beta_1 \left(\hat{T}_s - \hat{T}_\circ \right)}{\beta}$ non-linear convection parameter due to temperature, $\Pr = \frac{v_\circ \rho_\circ c_p}{k_\circ}$ is the Prandtl

number, and $M = \dfrac{\gamma\sigma_\circ T_{ref}}{\mu_\circ (bv_\circ)^{\frac{1}{2}}}$ is the thermocapillary parameter which is closely associated to the Marangoni number. In the present model the thickness of the liquid layer is of the order $\sqrt{\dfrac{v_\circ}{b}}$ hence Marangoni number based on this scale is given by $Ma = \dfrac{\gamma\sigma_\circ T_{ref}\left(\sqrt{\dfrac{v_\circ}{b}}\right)\rho_\circ c_p}{\mu_\circ k_\circ} = \Pr.M$

Local skin friction coefficient $\left(C_f\right)$ and local Nusselt number $\left(Nu_x\right)$ can be expressed as:

$$C_f = \frac{2(\tau_s)}{\left(\rho\hat{U}^2\right)} = -2e^{(A)} f''(0).\left(\mathrm{Re}_x^{-\frac{1}{2}}\right) \tag{22}$$

$$N\hat{u}_x = -\frac{x}{\hat{T}_{ref}}\left(\frac{\partial\hat{T}}{\partial y}\right)_{y=0} = \frac{1}{2\sqrt{(1-\alpha t)}}\theta'(0)\left(\mathrm{Re}_x^{3/2}\right) \tag{23}$$

3. Discussion of results

The nonlinear ODE's (16) and (17) subjected to the boundary conditions (18)-(21) are solved via enforcing Runge-Kutta and Newton's methods. To obtain numerical results we considered the non-dimensional values as $S = M = A = 1, \Pr = 2, \delta = 0.2, \lambda = 0.2, \lambda_1 = 0.5, \beta = 6, \zeta = 0.5$ these values were preserved constant in the entire study expect variations in the respective table(1and 2) and figures (2-11). To verify the accuracy of the obtained result comparison of the present results with the available literature is listed in Table 3. Comparative plots are presented considering non-linear convection (solid green line) and linear convection (dashed blue line) in Fig. 2- Fig. 11 for velocity and temperature profiles with respect to the pertinent parameters. From Fig. 2 it is evident that improvements in variable viscosity parameter (A) give rise to velocity and associated boundary layer thickness in both linear and nonlinear convection case. However, velocity boundary layer profiles are higher in nonlinear convection case compared to linear convection. As expected in Fig. 3 it is observed that improvement in A reduces temperature and associated boundary layer thickness in both linear and nonlinear convection case. In Fig. 4 and Fig. 5 it is apparent that augmentation in unsteadiness parameter (S) declines the momentum and thermal boundary layers. As anticipated, buoyancy effects acts on the flow which causes depreciation in velocity and thermal boundary layer. Thus non linear convection case shows higher momentum and thermal boundary layer profile compared to linear convection. In Fig .6 and Fig. 7 it is observed that improvement in thermal conductivity parameter (δ) lower the momentum and thermal boundary layer.

Comparatively, in nonlinear convection influence of δ is less. In Fig. 8 and Fig. 9 it is observed that improvement in Prandtl number (Pr) thickness of the thin film is approximately neglected thus there is decline in momentum and thermal boundary layer. However, nonlinear convection is less influenced by the increment in Pr compared to linear case. Augment in thermocapillary parameter (M) improves velocity and temperature associated boundary layer which is apparently noticed in Fig. 10 and Fig. 11. Further, it is visible that in case of nonlinear convection boundary layer thickness is high compared to linear convection.

From Table 1 and 2 it is observed that increasing values of the parameter A and Pr improves surface skin friction coefficient in both linear and nonlinear convection case. As the A values increases heat transfer rate decreases in both the case. Increment in S, δ and M reduces heat transfer rate in both linear and nonlinear convection case. Increment in S improves friction coefficient in nonlinear case and reduces in linear convection case. Increment in δ reduces friction coefficient for nonlinear convection and shows mixed performance in linear convection. Initially friction coefficient increases as δ grows friction coefficient reduces. Rising values of M declines skin friction in both linear and nonlinear convection case.

Elapsed time is more in nonlinear convection for growing values of A, δ, Pr and M compared to linear convection. However, for growing values of S nonlinear convection takes less elapsed time compared to linear convection.

4. Conclusion

Flow of a thin liquid film and heat transfer over the surface of unsteady stretching sheet is modeled in the current investigation. It is found that non-linear convection case shows higher velocity and associated boundary layer thickness compared with linear convection whereas linear convection case shows higher temperature and associated boundary layer thickness for the improvement in values of variable viscosity parameter, unsteadiness parameter, thermal conductivity parameter, Prandtl number,thermocapillary parameter. Elapsed time is more in nonlinear convection for growing values of A, δ, Pr and M compared to linear convection. Increment in S, δ and M reduces heat transfer rate in both linear and nonlinear convection case.

5. References

[1]. Crane L J 1970 Flow past a stretching plate *ZAMP* pp 21645-647

[2]. Hayat T, M. Farooq M, A. Alsaedi A, and Al-Solamy F 2015 Impact of Cattaneo-Christov heat flux in the flow over a stretching sheet with variable thickness. *AIP Advances*, 5 pp 087159

[3]. Rashidi M M, Ganesh N V, Hakeem A A, and Ganga B 2014 Buoyancy effect on MHD flow of nanofluid over a stretching sheet in the presence of thermal radiation *Journal of Molecular Liquids* 198 pp 234-238.

[4]. Majeed A, Zeeshan A, Alamri S Z, and Ellahi R 2018 Heat transfer analysis in ferromagnetic viscoelastic fluid flow over a stretching sheet with suction *Neural Computing and Applications* 30 pp 1947-1955.

[5]. Harmindar S Takhar, Ali J Chamkha, Girishwar Nath 2000 Flow and mass transfer on a stretching sheet with a magnetic field and chemically reactive species,12 pp1303-1314.

[6]. Raju C S K, Sandeep N, Sulochana C, Sugunamma V, JayachandraBabu M 2015 Radiation, inclined magnetic field and cross-diffusion effects on flow over a stretching surface *Journal of the Nigerian Mathematical Society*, 34pp 169-180.

[7]. Aziz M M 2013 Mixed convection flow of a micropolar fluid from an unsteady stretching surface with viscous dissipation *Journal of the Egyptian Mathematical Society* 21 pp 385-394.

[8]. Makinde O D 2013 Computational modelling of nanofluids flow over a convectively heated unsteady stretching sheet *Current Nanoscience*, 9 pp 673-678.

[9]. Jayachandra Babu M, Sandeep N 2016 Three-dimensional MHD slip flow of nanofluids over a slendering stretching sheet with thermophoresis and Brownian motion effects *Adv. Powder Technology* 27 pp 2039–2050. doi:10.1016/j.apt.2016.07.013.

[10]. Raju C S K, Sandeep N, Babu M J 2016 Effects of non-uniform heat source/sink and chemical reaction on unsteady MHD nanofluid flow over a permeable stretching surface *Adv. Sci. Eng. Med.* 8 pp 165–174.

[11]. Rahimi J, Ganji D D, Khaki M, Hosseinzadeh K 2016 Solution of the boundary layer flow of an Eyring-Powell non-Newtonian fluid over a linear stretching sheet by collocation method *Alexandria Eng. J*. pp 4–10. doi:10.1016/j.aej.2016.11.006.

[12]. Junaid Ahmed Khan, Mustafa M, Hayat T, Alsaedi A 2015 Numerical study of Cattaneo-Christov Heat flux Model for Viscoelastic flow Due to an Exponentially Stretching Surface *Plos One* 10pp e0137363.

[13]. Vajravelu K, Nayfeh J 1972 Hydromagnetic flow of a dusty fluid over a stretching sheet *International Journal of linear Mech* 27 pp 937-945.

[14]. Mamatha S U, Mahesha, Raju C S K 2017 Cattaneo-Christov on heat and mass transfer of unsteady Eyring Powell dusty nanofluid over sheet with heat and mass flux conditions *Informatics Med. Unlocked* 9 pp 76–85 doi:10.1016/j.imu.2017.06.001

[15]. Khan I, Malik M Y, Salahuddin T, Khan M, and Rehman K U 2018 Homogenous–heterogeneous reactions in MHD flow of Powell–Eyring fluid over a stretching sheet with Newtonian heating *Neural Computing and Applications* 30 pp 3581-3588.

[16]. Wang C Y 1990 Liquid film on an unsteady stretching surface, *Q Appl Math*, 48 pp 601-10.

[17]. Aziz R C, Hashim I, Abbasbandy S 2018 Flow and Heat Transfer in a Nanofluid Thin Film over an Unsteady Stretching Sheet *Sains Malaysiana* 47pp 1599-1605.

[18]. Faraz N, and Khan Y 2018 Thin film flow of an unsteady Maxwell fluid over a shrinking/stretching sheet with variable fluid properties *International Journal of Numerical Methods for Heat & Fluid Flow*, 28 pp1596-1612.

[19]. Dandapat B S , Santra B, Vajravelu K 2007 The effects of variable fluid properties and thermocapillarity, on the flow of a thin film on an unsteady stretching sheet *International Journal of Heat and Mass Transfer* 50 pp 991–996.

[20]. Khader M M 2018 Numerical study for the BVP of the liquid film flow over an unsteady stretching sheet with thermal radiation and magnetic field *Boundary Value Problems*, pp77.

[21]. Sandeep N 2017 Effect of aligned magnetic field on liquid thin film flow of magnetic-nanofluids embedded with graphene nanoparticles *Advanced Powder Technology*, 28 pp 865-875.

[22]. Mamatha Upadhya S, Raju CSK, Saleem S 2018 Nonlinear unsteady convection on micro and nanofluids with Cattaneo-Christov heat flux *Results in Physics*, 9 pp 779-786.

[23]. Shehzad S A, Abbasi F M, Hayat T, Alsaedi A 2016 Cattaneo-Christov heat flux model for Darcy-Forchheimer flow of an Oldroyd-B fluid with variable conductivity and non-linear convection *J. Mol. Liq*. 224 pp 274–278. doi:10.1016/j.molliq.2016.09.109

[24]. Kumar R and Sood S 2015 Nonlinear convection stagnation point heat transfer and MHD fluid flow in porous medium towards a permeable shrinking sheet *arXiv preprint arXiv:*1511.06109

[25]. Qayyum S, Hayat T, Shehzad S A, Alsaedi A 2017 Nonlinear convective flow of Powell-Erying magneto nanofluid with Newtonian heating *Results in Physics* 7 pp2933-2940. doi:http://dx.doi.org/10.1016/j.rinp.2017.08.001

[26]. Idrees M , Sajid Rehman ,Rehan Ali Shah ,M. Ullah ,Tariq Abbas 2018 A similarity solution of time dependent MHD liquid film flow over stretching sheet with variable physical properties *Results in Physics*, 8 pp 194–205.

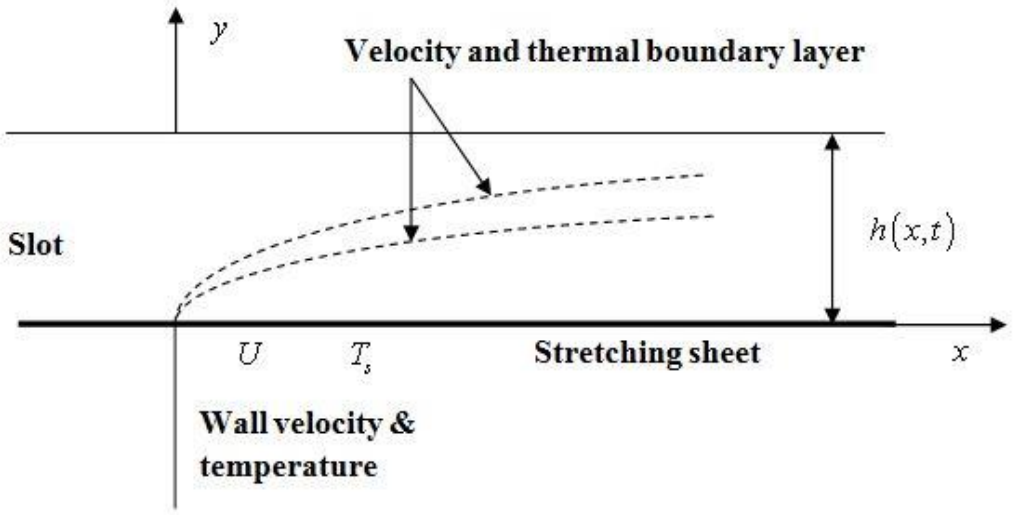

Figure 1. Flow configuration and coordinate system.

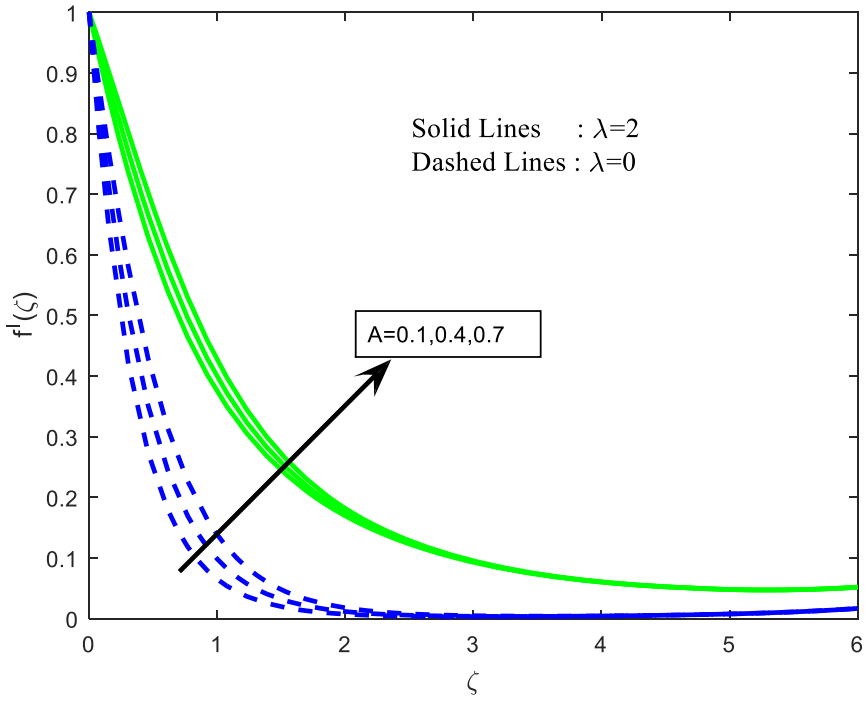

Figure 2. Influence of variable viscosity parameter on velocity profiles.

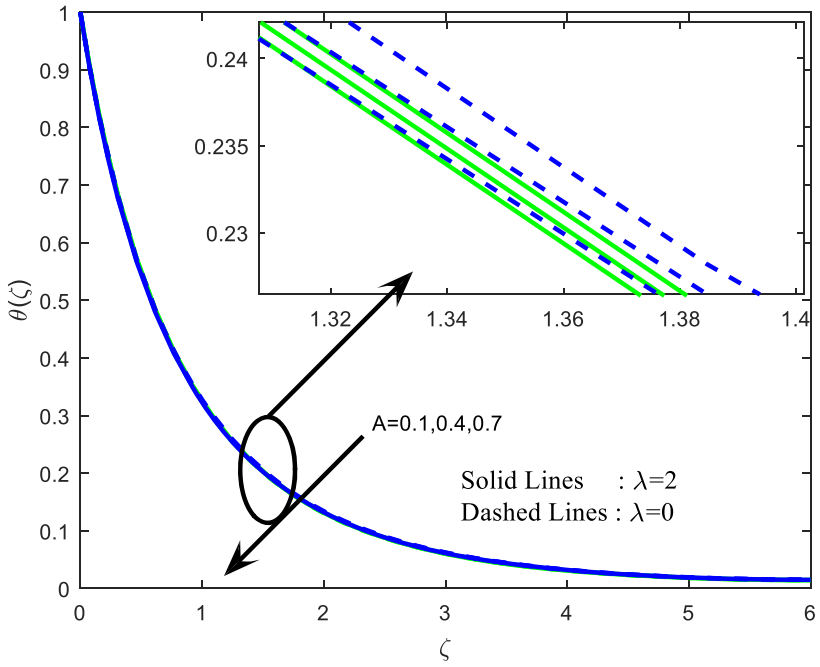

Figure 3. Influence of variable viscosity parameter on temperature profiles

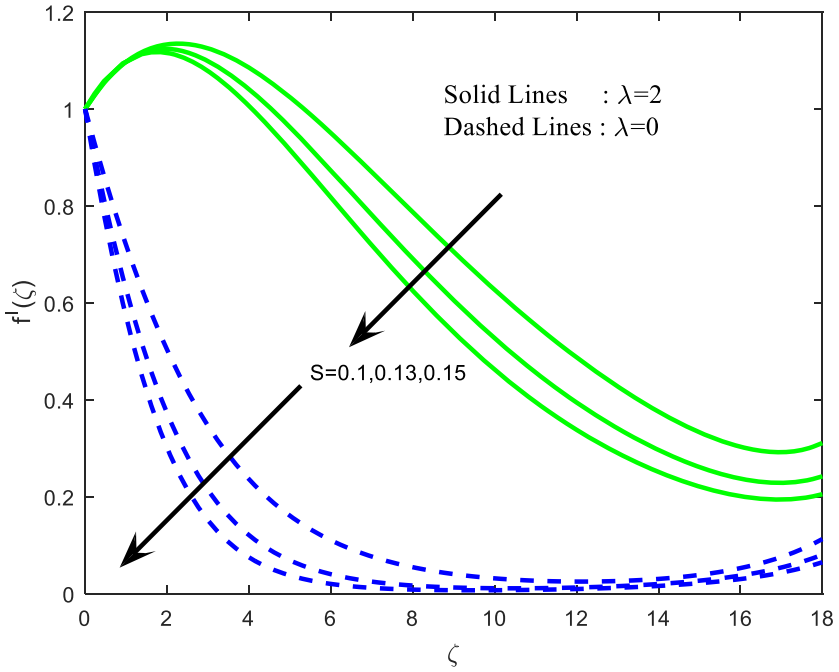

Figure 4. Influence of unsteadiness parameter on velocity profiles

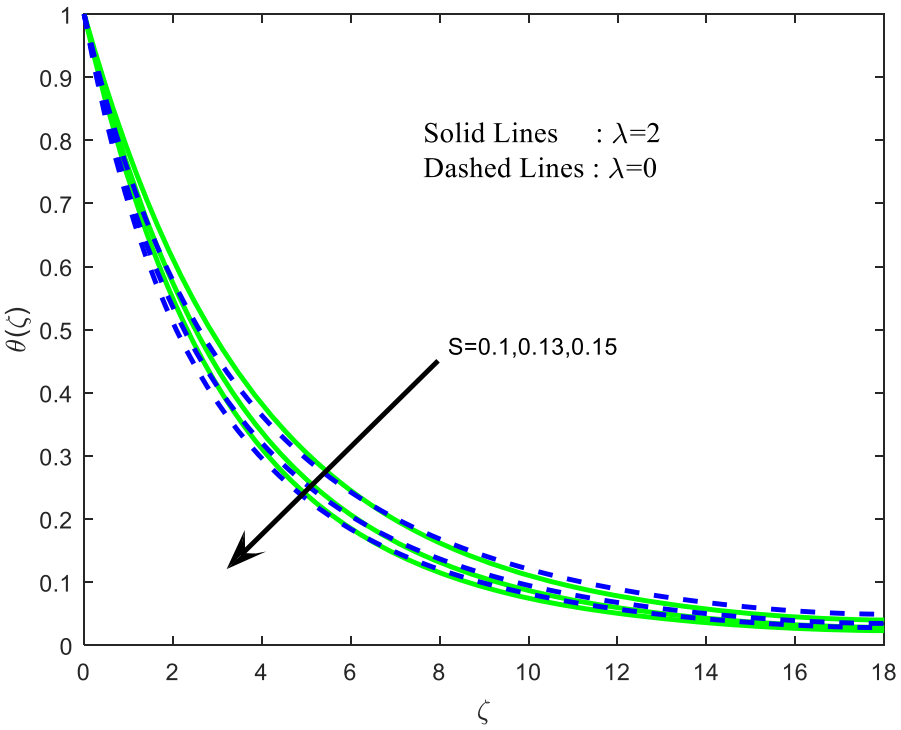

Figure 5. Influence of unsteadiness parameter on temperature profiles

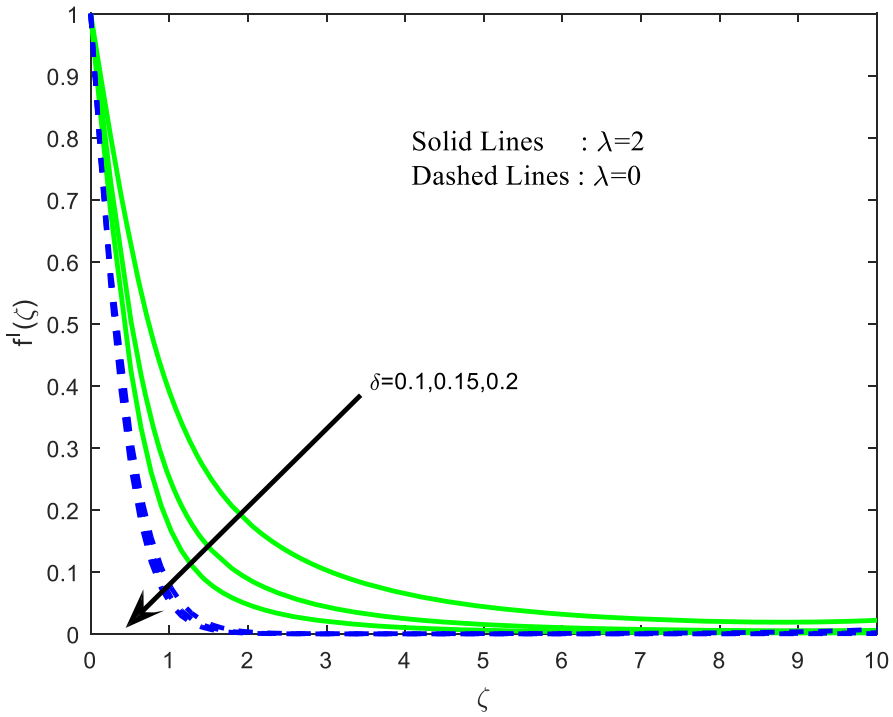

Figure 6. Influence of thermal conductivity parameter on velocity profiles

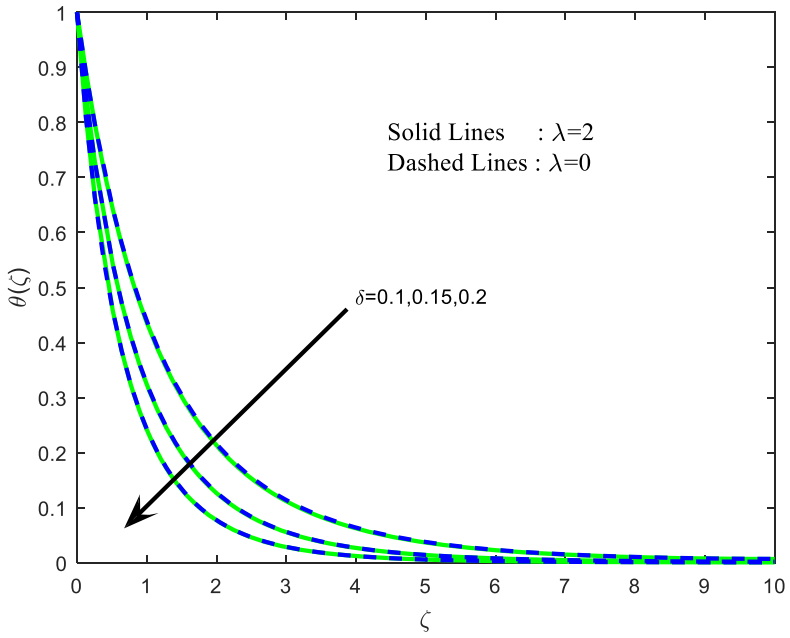

Figure 7. Influence of thermal conductivity parameter on temperature profiles

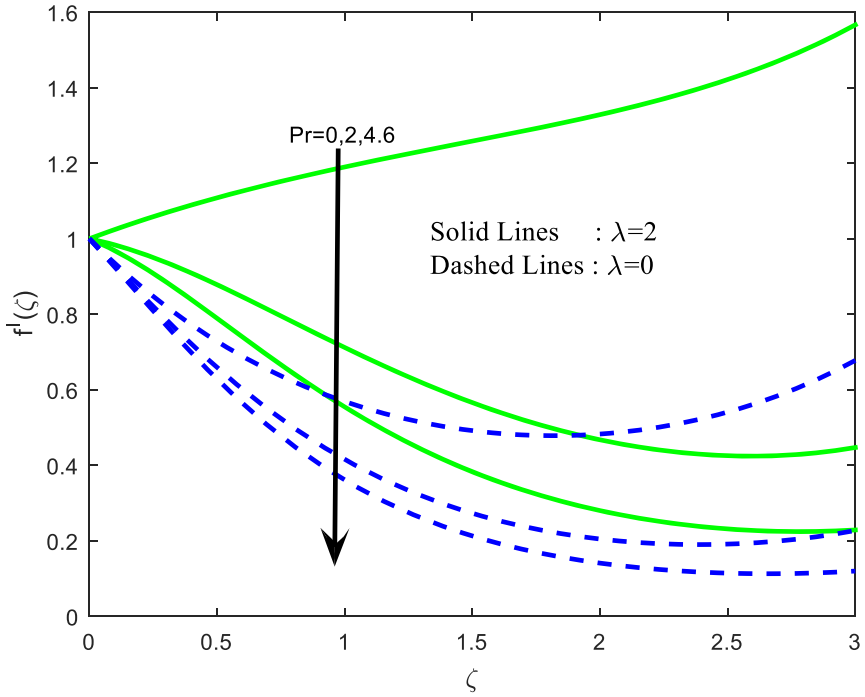

Figure 8. Influence of Prandtl number on velocity profiles

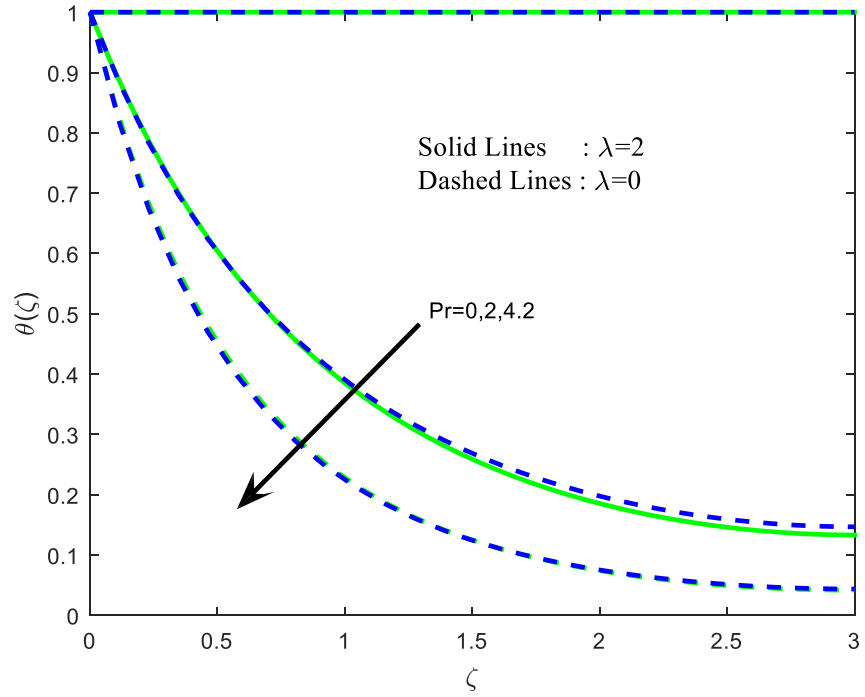

Figure 9. Influence of Prandtl number on temperature profiles

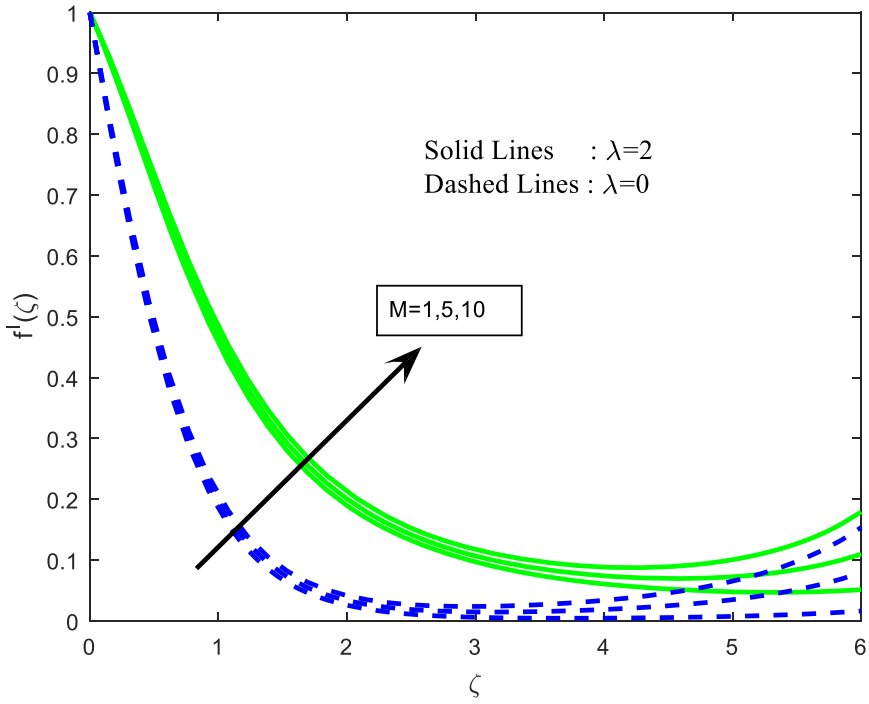

Figure 10. Influence of thermocapillary parameter on velocity profiles

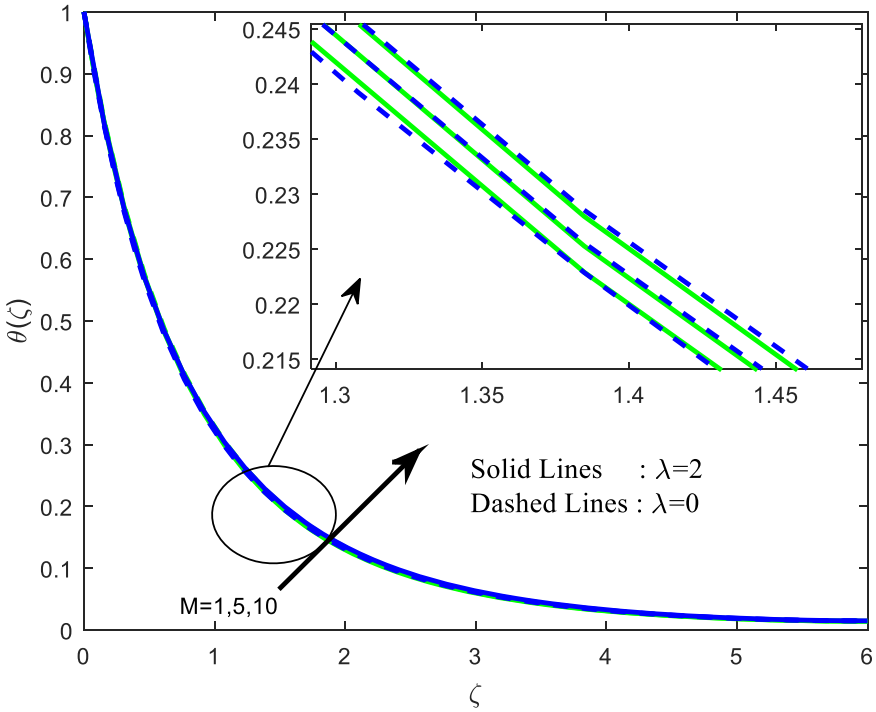

Figure 11. Influence of thermocapillary parameter on temperature profiles.

Table1: Variation in friction factors and local Nusselt number with elapsed time for $\lambda = 2$ case.

A	S	δ	Pr	M	$f''(0)$	$-\theta'(0)$	elapsed time (seconds)
0.1					1.400494	1.146725	0.724367
0.4					2.001803	1.249540	
0.7					2.579293	1.248175	
	0.1				0.272888	0.777628	0.819657
	0.13				0.437353	0.578285	
	0.15				0.486495	0.561478	
		0.1			1.622001	0.777317	0.764166
		0.15			1.112011	0.489949	
		0.2			0.870468	0.343105	
			0.2		-1.242813	2.000000	0.540468
			4		1.161554	1.701423	
			6		2.118035	1.545511	
				1	3.266144	1.247051	0.679891
				5	3.002355	0.968372	
				10	2.717089	0.828890	

Table 2: Variation in friction factors and local Nusselt number with elapsed time for $\lambda = 0$ case.

A	S	δ	Pr	M	$f''(0)$	$-\theta'(0)$	elapsed time (seconds)
0.1					1.073486	0.968562	0.621407
0.4					2.459396	1.139764	
0.7					3.456127	1.135345	
	0.1				0.508891	0.739725	1.050721
	0.13				0.391531	0.652553	
	0.15				0.301575	0.603536	
		0.1			0.571476	0.713034	0.673816
		0.15			0.455163	0.492806	
		0.2			0.586461	0.401533	
			0.2		3.225215	2.000000	0.501422
			4		3.785686	1.566158	
			6		4.171688	1.347270	
				1	5.125923	1.235847	0.578252
				5	3.750183	0.960244	
				10	2.957615	0.823487	

Table 3: Comparison of the values for $Ma = \lambda = \lambda_1 = 0$ with varying values of S

	Idrees et al. [26]		Present results	
S	$f''(0)$	$-\theta'(0)$	$f''(0)$	$-\theta'(0)$
0.4	-0.015803	3.10843	-0.015803	3.10843
0.6	-0.008893	3.52120	-0.008883	3.52220
0.8	-0.006643	3.73098	-0.006643	3.73088
1.0	-0.004758	3.97183	-0.004778	3.97183
1.2	-0.005376	3.88348	-0.005476	3.88368
1.4	-0.006479	3.74892	-0.006579	3.74891